COBEM 2023 27TH INTERNATIONAL CONGRESS OF MECHANICAL ENGENEERING

ABCM Brazilian Society of Mechanical Sciences and Engineering
27th ABCM International Congress of Mechanical Engineering
December 04-08, 2023, Florianópolis-SC, Brazil

COB-2023-2368
ESTIMATION OF SPATIALLY VARYING THERMAL CONTACT CONDUCTANCES IN DUAL LAYER PIPES USING THE RECIPROCITY FUNCTIONAL APPROACH

Carlos Eduardo Polatschek Kopperschmidt
Bruno Henrique Marques Margotto
Marcelo José Colaço
Federal University of Rio de Janeiro, UFRJ, Technology Center, Bloco G – Cidade Universitária da UFRJ, Ilha do Governador, Rio de Janeiro/RJ, 21941-909, Brazil.
cadupolkop@mecanica.coppe.ufrj.br, brunohmmargotto@mecanica.coppe.ufrj.br, colaco@ufrj.br

Wellington Betencurte da Silva
Federal University of Espírito Santo, UFES. Alto Universitário, Guararema, Alegre/ES, 29.500-999, Brazil.
wellingtonufes@gmail.com

Abstract. *Thermal contact conductances (TCC) play a critical role in various engineering applications involving heat transfer between solid surfaces. The proper knowledge of TCC is required in many engineering applications, such as electronic packaging, nuclear reactors, aerospace, and biomedicine applications, among others, where some careful evaluation of TCC allows a more accurate analysis of the correspondent thermal system, leading to improved efficiency, reduced energy consumption, and prevention of thermal damage. In addition, TCC estimation allows a qualitative assessment regarding the presence of discontinuities or failures within the material. The Reciprocity Functional Method (RFM), coupled with the Classical Integral Transform Technique (CITT), has been used as a promising tool for TCC estimation, as it allows the solution of inverse boundary value problems with low computational cost, not requiring iterative methods nor intrusive measurements, working as a nondestructive testing to investigate interfacial flaws between solid materials. The technique defines two auxiliary problems: one for the temperature discontinuity and the other for the interfacial heat flux, both on the inaccessible interface between the composite materials. In this work, the RFM and the CITT were used to estimate different types of TCCs, considering a three-dimensional double-layer hollow cylinder geometry, which could represent, for instance, double-layer pipelines found in the oil industry. Temperature measurements for the inverse problem were considered available on the outer surface of the pipe, and the results showed good estimates for different cases, even using high noise levels in the measurements.*

Keywords: *Reciprocity functional, inverse heat conduction problem, thermal contact conductance, classical integral transform technique*

1. INTRODUCTION

Failures in contact materials have significant implications in various applications, including nuclear-reactor cooling (Milosevic et. al, 2002), aerodynamic heating of supersonic aircraft and missiles (Guilmore, 2002), packaging of electronics (Cui et. al 2014), biomedical engineering (McWaid and Marshall, 1992), combustion engines (Goudarzi et al., 2015), thermoelectric generators (Karthick et al., 2019), battery systems with parallel-connected cells (Fill et al., 2020), and more. The effectiveness of these materials relies heavily on the contact between their different layers.

One crucial parameter for evaluating a contact interface is the thermal contact conductance (TCC), which is defined as the ratio between the heat flux and the temperature jump at the contacting interface (Özisik, 1993). This parameter provides valuable insights regarding the heat transfer efficiency between the composite layers, being essential for the design and performance evaluation of composite materials.

In practical problems, estimating TCC often involves experimental procedures that require intrusive techniques. These methods demand knowledge of the surface profile between the materials, including their roughness and interfacial temperature. Consequently, they may not be applicable to certain equipment or scenarios that require only non-intrusive measurements, such as dual layer pipelines. Alternatively, some approaches, like in Loulou and Scott (2006), aim to estimate the TCC through a non-intrusive, however iterative method, which can be very time-consuming.

Another method that has been used to estimate TCC is the artificial neural networks (ANN), as demonstrated by Goudarzi et. al (2015). However, the training stage of such method requires a substantial amount of complementary data and demands considerable time and computational resources.

To address this limitation, Colaço and Alves (2012) proposed a non-intrusive and non-iterative approach to solving a two-dimensional steady-state inverse problem for estimating unknown TCC profiles at the interface between two solid

materials. Their method combined the reciprocity functional approach (RF) with the method of fundamental solutions (MFS), providing a promising alternative that resulted in an accurate TCC estimation without the need of intrusive measurements. The concept of the reciprocity gap functional was introduced by Andrieux and Abda (1993), based on the Maxwell-Betti reciprocity theorem. The key concept concerns the fact that a field in equilibrium within a material body exhibits distinct responses when perturbed, depending on the presence of absence of discontinuities inside the body.

This approach has been demonstrated to be computationally efficient and accurate, and it has undergone further advancements to enhance its capabilities. These improvements include the estimation of TCC using transient measurements (Colaço *et al*., 2014), the estimation of transient TCC profiles (Colaço and Alves, 2015), and the combination of the method with the Classical Integration Transform Technique (CITT) (Padilha et. al, 2016). This combination of RF with CITT reduced the inverse problem solution to a straightforward algebraic equation. These developments have expanded the applicability and versatility of the method, making it a powerful tool for estimating thermal contact conductance in various scenarios.

While the previous works utilizing the RF method for TCC estimation have focused on rectangular systems, the present work focus on cylindrical coordinates. This extension to cylindrical coordinates would allow the analyses of pipelines made of composite materials, possibly identifying contacting flaws between the different layers.

2. PHYSICAL PROBLEM

The physical problem involves a three-dimensional steady-state heat transfer problem of two concentric tubes (Ω_1 and Ω_2) with an interface surface (Γ_1). The Ω_1 and Ω_2 materials are considered isotropic, with constant thermal conductivities, k_1 and k_2, respectively.

The outer tube is subjected to a convective heat transfer with the environment at Γ_2, where the environment is assumed to have a constant temperature T_∞. On the other hand, the inner tube is subjected to a prescribed temperature boundary condition at Γ_0.

On the contact surface Γ_1 between the two tubes, a Robin boundary condition is applied, where h_{ctc} represents the thermal contact conductance (TCC). Additionally, the normal heat flux continuity condition is enforced on the interface to ensure that heat transfer is continuous between the two contacting solids.

The upper and bottom surfaces of both materials, denoted as S_0 and S_1, respectively, are assumed to be thermally insulated. The schematic representation of the proposed problem is illustrated in Figure 1.

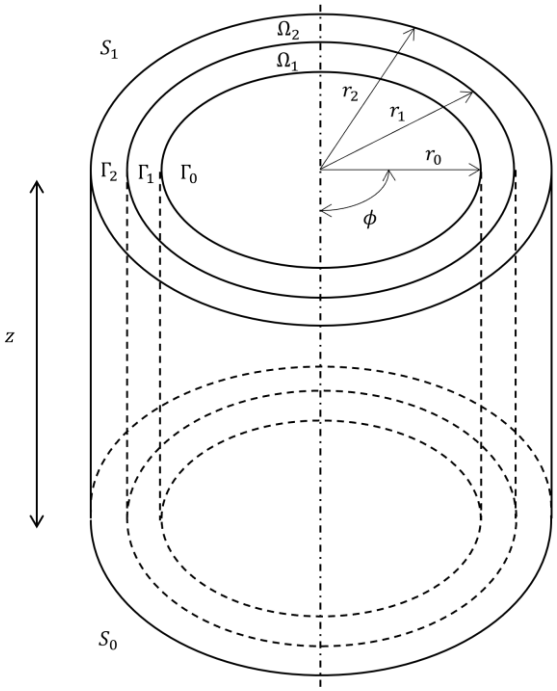

Figure 1. Physical problem scheme.

The mathematical formulation is given by the direct problem described by the Eqs. (1)-(10).

$$\frac{\partial^2 T_1}{\partial r^2} + \frac{1}{r}\frac{\partial T_1}{\partial r} + \frac{1}{r^2}\frac{\partial^2 T_1}{\partial \phi^2} + \frac{\partial^2 \mathrm{T}_1}{\partial \mathrm{Z}^2} = 0, \text{ in } \Omega_1 \tag{1}$$

$$\frac{\partial^2 T_2}{\partial r^2} + \frac{1}{r}\frac{\partial T_2}{\partial r} + \frac{1}{r^2}\frac{\partial^2 T_2}{\partial \phi^2} + \frac{\partial^2 \mathrm{T}_2}{\partial \mathrm{Z}^2} = 0, \text{ in } \Omega_2 \tag{2}$$

$$T = 0, \text{ on } \Gamma_0 \tag{3}$$

$$-k_1 \frac{\partial T_1}{\partial \mathbf{n}_1} = h_{\mathrm{TCC}}(T_1 - T_2), \text{ on } \Gamma_1 \tag{4}$$

$$k_1 \frac{\partial T_1}{\partial \mathbf{n}_1} = -k_2 \frac{\partial T_2}{\partial \boldsymbol{n}_2}, \text{ on } \Gamma_1 \tag{5}$$

$$-k_2 \frac{\partial T_2}{\partial \mathbf{n}_2} = h_2(T_2 - T_\infty), \text{ on } \Gamma_2 \tag{6}$$

$$\frac{\partial T_1}{\partial \mathbf{n}_1} = 0, \text{ on } S_0 \tag{7}$$

$$\frac{\partial T_1}{\partial \mathbf{n}_1} = 0, \text{ on } \mathrm{S}_1 \tag{8}$$

$$\frac{\partial T_2}{\partial \mathbf{n}_2} = 0, \text{ on } S_0 \tag{9}$$

$$\frac{\partial T_2}{\partial \mathbf{n}_2} = 0, \text{ on } \mathrm{S}_1 \tag{10}$$

This work proposes the estimation of the TCC, described as h_{ctc} in Eq. (4), which is supposed to be unknown, representing an inverse problem (Özisik, 1993). The complementary data for the inverse problem are given by measurements Y taken on the externally accessible boundary Γ_2, possibly using an infrared camera.

3. INVERSE PROBLEM

The inverse problem consists of the estimation of the thermal contact conductance (h_{ctc}) using the reciprocity functional method, as defined by Colaço and Alves (2012), which requires two auxiliary problems. The first auxiliary problem aims to estimate the temperature jump across the interface Γ_1, denoted as $\Delta T_{\Gamma_1}[°\mathrm{C}]$ (also referred to as the "temperature discontinuity"), where $\Delta T = (T_1 - T_2)$. The second auxiliary problem focuses on estimating the heat flux, represented as $q_{\Gamma_1}[\mathrm{W/m^2}]$, also across the same interface Γ_1.

Subsequently, the results obtained from solving these two auxiliary problems are combined to obtain the distribution of thermal contact conductance along the interface Γ_1, where $h_{ctc}[\mathrm{W/m^2K}] = q_{\Gamma_1}/\Delta T_{\Gamma_1}$.The procedure employed to describe ΔT_{Γ_1} and q_{Γ_1}, considering the two auxiliary problems, is detailed in the subsequent sections of the paper.

3.1 First auxiliary problem

The first auxiliary problem aims the estimation of ΔT_{Γ_1}, the temperature jump at the interface Γ_1, and is described by Eqs. (11)-(20). Notice that F is an auxiliary function and the subindex 1 and 2 describe $F_{1,p} \in C^2(\Omega_1)$ and $F_{2,p} \in C^2(\Omega_2)$, respectively. The orthonormal basis system $\psi_p(\phi, z) \in L^2(\Gamma_2)$ is chosen to take advantage of its orthogonal properties.

$$\frac{\partial^2 F_{1,p}}{\partial r^2} + \frac{1}{r}\frac{\partial F_{1,p}}{\partial r} + \frac{1}{r^2}\frac{\partial^2 F_{1,p}}{\partial \phi^2} + \frac{\partial^2 F_{1,\mathrm{p}}}{\partial \mathrm{Z}^2} = 0, \text{ in } \Omega_1 \tag{11}$$

$$\frac{\partial^2 F_{2,p}}{\partial r^2} + \frac{1}{r}\frac{\partial F_{2,p}}{\partial r} + \frac{1}{r^2}\frac{\partial^2 F_{2,p}}{\partial \phi^2} + \frac{\partial^2 F_{2,\mathrm{p}}}{\partial \mathrm{Z}^2} = 0, \text{ in } \Omega_2 \tag{12}$$

$$F_{1,p} = 0, \text{ on } \Gamma_0 \tag{13}$$

$$F_{1,p} = F_{2,p}, \text{ on } \Gamma_1 \tag{14}$$

$$k_1 \frac{\partial F_{1,p}}{\partial \mathbf{n}_1} = -k_2 \frac{\partial F_{2,p}}{\partial \mathbf{n}_2}, \text{ on } \Gamma_1 \tag{15}$$

$$F_{2,p} = \psi_p(\phi, z), \text{ on } \Gamma_2 \tag{16}$$

$$\frac{\partial F_{1,p}}{\partial \mathbf{n_1}} = 0, \text{ on } S_0 \tag{17}$$

$$\frac{\partial F_{1,p}}{\partial \mathbf{n_1}} = 0, \text{ on } S_1 \tag{18}$$

$$\frac{\partial F_{2,p}}{\partial \mathbf{n_2}} = 0, \text{ on } S_0 \tag{19}$$

$$\frac{\partial F_{2,p}}{\partial \mathbf{n_2}} = 0, \text{ on } S_1 \tag{20}$$

The solution of the first auxiliary problem is obtained by using the CITT and is given by Eqs. (21) and (22), where the eigenvalues η_m are positive roots of $\sin \eta_m L = 0$.

$$F_{1,p}(r,\phi,z) = \frac{1}{L}\left(\frac{1}{2\pi}\bar{\bar{F}}_{1,p}(r,0,\eta_0) + \sum_{\nu=1}^{\infty}\frac{1}{\pi}\bar{\bar{F}}_{1,p}(r,\nu,\eta_0)\right) + \sum_{m=1}^{\infty}\frac{2}{L}\cos\eta_m z\left(\frac{1}{2\pi}\bar{\bar{F}}_{1,p}(r,0,\eta_m) + \sum_{\nu=1}^{\infty}\frac{1}{\pi}\bar{\bar{F}}_{1,p}(r,\nu,\eta_m)\right) \tag{21}$$

$$F_{2,p}(r,\phi,z) = \frac{1}{L}\left(\frac{1}{2\pi}\bar{\bar{F}}_{2,p}(r,0,\eta_0) + \sum_{\nu=1}^{\infty}\frac{1}{\pi}\bar{\bar{F}}_{2,p}(r,\nu,\eta_0)\right) + \sum_{m=1}^{\infty}\frac{2}{L}\cos\eta_m z\left(\frac{1}{2\pi}\bar{\bar{F}}_{2,p}(r,0,\eta_m) + \sum_{\nu=1}^{\infty}\frac{1}{\pi}\bar{\bar{F}}_{2,p}(r,\nu,\eta_m)\right) \tag{22}$$

The functions $\bar{\bar{F}}_{1,p}$ and $\bar{\bar{F}}_{2,p}$ are defined as the transformation of $F_{1,p}$ and $F_{2,p}$ in the ϕ and z directions, by the CITT procedure, and are given by Eqs. (23) and (24), where the coefficients $C_{1,2,\ldots,9}$ are described in Table 1 to simplify the expressions, and $\Delta k = (k_1 - k_2)$. The function $\bar{\bar{\psi}}_p$ gives the transformation of the orthonormal basis system ψ_p in the ϕ and z directions. J and Y represent the Bessel functions of first and second kind, respectively.

$$\bar{\bar{F}}_{1,p,k}(r,\nu,\eta) = \bar{\bar{\psi}}_p \frac{2k_2}{\pi}\frac{J_\nu(r\eta_m)Y_\nu(r_0\eta_m) - J_\nu(r_0\eta_m)Y_\nu(r\eta_m)}{J_\nu(r_1\eta_m)J_\nu(r_2\eta_m)Y_\nu(r_0\eta_m)C_1 - \Delta k\nu\, J_\nu(r_1\eta_m)^2 Y_\nu(r_0\eta_m)Y_\nu(r_2\eta_m) + Y_\nu(r_2\eta_m)C_2 + Y_\nu(r_1\eta_m)(C_3 + C_4)} \tag{23}$$

$$\bar{\bar{F}}_{2,p,k}(r,\nu,\eta) = \bar{\bar{\psi}}_p \frac{Y_\nu(r_1\eta_m)(J_\nu(r\eta_m)C_5 - Y_\nu(r\eta_m)C_6 + J_\nu(r\eta_m)C_7) + J_\nu(r_1\eta_m)(Y_\nu(r\eta_m)C_8 - J_\nu(r\eta_m)C_9)}{Y_\nu(r_1\eta_m)(J_\nu(r_2\eta_m)C_5 - Y_\nu(r_2\eta_m)C_6 + J_\nu(r_2\eta_m)C_7) + J_\nu(r_1\eta_m)(Y_\nu(r_2\eta_m)C_8 - J_\nu(r_2\eta_m)C_9)} \tag{24}$$

Table 2. Coefficients of Eqs. (23) and (24).

COEFFICIENTS	
$C_1 = r_1 k_2 \eta_m J_{\nu-1}(r_1\eta_m) + \Delta k\nu Y_\nu(r_1\eta_m)$	$C_6 = k_2 J_\nu(r_0\eta_m)(J_{\nu-1}(r_1\eta_m) - J_{\nu+1}(r_1\eta_m))$
$C_2 = r_1\Delta k\eta_m J_{\nu-1}(r_1\eta_m)Y_\nu(r_0\eta_m) + J_\nu(r_0\eta_m)(\Delta k\nu Y_\nu(r_1\eta_m) - r_1 k_1 \eta_m Y_{\nu-1}(r_1\eta_m))$	$C_7 = \Delta k J_\nu(r_0\eta_m)(Y_{\nu-1}(r_1\eta_m) - Y_{\nu+1}(r_1\eta_m))$
$C_3 = J_\nu(r_0\eta_m)\left(\Delta k J_\nu(r_2\eta_m)(r_1\eta_m Y_{\nu-1}(r_1\eta_m) - \nu Y_\nu(r_1\eta_m))\right)$	$C_8 = k_1 J_\nu(r_0\eta_m)(Y_{\nu-1}(r_1\eta_m) - Y_{\nu+1}(r_1\eta_m)) - \Delta k(J_{\nu-1}(r_1\eta_m) - J_{\nu+1}(r_1\eta_m))Y_\nu(r_0\eta_m)$
$C_4 = r_1\eta_m J_{\nu-1}(r_1\eta_m)(k_2 Y_\nu(r_2\eta_m) - k_1 J_\nu(r_2\eta_m)Y_\nu(r_0\eta_m))$	
$C_5 = k_1(J_{\nu-1}(r_1\eta_m) - J_{\nu+1}(r_1\eta_m))Y_\nu(r_0\eta_m)$	$C_9 = k_2 Y_\nu(r_0\eta_m)(Y_{\nu-1}(r_1\eta_m) - Y_{\nu+1}(r_1\eta_m))$

To estimate the temperature jump on the contacting interface, it is necessary to multiply Eq. (1) by F_1 and Eq. (11) by $-T_1$, add them together and integrate the result over the domain Ω_1. The same procedure is used for Ω_2. Then, using Green's second identity, considering the boundary conditions of the physical problem given by Eqs. (3)-(10), and the boundary conditions of the first auxiliary problem given by Eqs. (13)-(20), the resulting expression, as in Colaço and Alves (2012), is given by:

$$k_2 \int_{\Gamma_2}\left[F_{2,p}\frac{h_2}{k_2}(Y - T_\infty) - Y\frac{\partial F_{2,p}}{\partial \boldsymbol{n_2}}\right]d\Gamma_2 = -\int_{\Gamma_1}\left[k_1\frac{\partial F_{1,p}}{\partial \boldsymbol{n_1}}(T_1 - T_2)\right]d\Gamma_1 \tag{25}$$

The left side of Eq. (25) is defined as $k_2\mathcal{R}(F_{2,p,k})$, where $\mathcal{R}(\ )$ is the reciprocity functional. Then, it is possible to rewrite this expression as:

$$k_2\mathcal{R}(F_{2,p}) = \langle k_1\frac{\partial F_{1,p}}{\partial \boldsymbol{n_1}}, (T_1 - T_2)\rangle_{\Gamma_1} \tag{26}$$

From Eq. (26), we assume that $(T_1 - T_2)$ can be written as a linear combination of the orthogonal functions β_i, as described in Eq. (27), where β_i is defined as in Eq.(28), and α_i are the weighting coefficients to be determined.

$$(T_1 - T_2)_{\Gamma_1} = \sum_{i=1}^{N} \alpha_i \beta_i \tag{27}$$

$$\beta_i = \left(k_1 \frac{\partial F_{1,i}}{\partial \mathbf{n}_1}\right)_{\Gamma_1} \tag{28}$$

Then, combining Eqs. (26) and (27) we can write the following linear system to determine α_i:

$$k_2 \mathcal{R}(F_{2,p}) = \sum_{i=1}^{N} \alpha_i \langle \beta_i, \beta_p \rangle_{\Gamma_1} \tag{29}$$

Once α_i is found, ΔT_{Γ_1} can be determined directly from Eq. (27).

3.2 Second auxiliary problem

The second auxiliary problem aims the estimation of q_{Γ_1}, the interfacial heat flux, and is described by Eqs. (30)-(34). Notice that G is an auxiliary function and the index 2 describe $G_{2,p} \in C^2(\Omega_2)$. The orthonormal basis system $\xi_p(\phi, z) \in L^2(\Gamma_2)$ is chosen to take advantage of its orthogonal properties.

$$\frac{\partial^2 G_{2,p}}{\partial r^2} + \frac{1}{r}\frac{\partial G_{2,p}}{\partial r} + \frac{1}{r^2}\frac{\partial^2 G_{2,p}}{\partial \phi^2} + \frac{\partial^2 G_{2,\mathrm{p}}}{\partial \mathrm{Z}^2} = 0, \text{ in } \Omega_2 \tag{30}$$

$$\frac{\partial G_{2,p}}{\partial \mathbf{n}_2} = 0, \text{ on } \Gamma_1 \tag{31}$$

$$G_{2,p} = \xi_p(\phi, z), \text{ on } \Gamma_2 \tag{32}$$

$$\frac{\partial G_{2,p}}{\partial \mathbf{n}_2} = 0, \text{ on } S_0 \tag{33}$$

$$\frac{\partial G_{2,p}}{\partial \mathbf{n}_2} = 0, \text{ on } S_1 \tag{34}$$

The solution of the second auxiliary problem is obtained by using the CITT and is given by Eq. (35), where the eigenvalues η_m are the positive roots of $\sin \eta_m L = 0$.

$$G_{2,p}(r, \phi, z) = \frac{1}{\mathrm{L}}\left(\frac{1}{2\pi}\bar{\bar{G}}_{2,p}(r, 0, \eta_0) + \sum_{\nu=1}^{\infty}\frac{1}{\pi}\bar{\bar{G}}_{2,p}(r, \nu, \eta_0)\right) + \sum_{\mathrm{m}=1}^{\infty}\frac{2}{\mathrm{L}}\cos \eta_m z \left(\frac{1}{2\pi}\bar{\bar{G}}_{2,p}(r, 0, \eta_m) + \sum_{\nu=1}^{\infty}\frac{1}{\pi}\bar{\bar{G}}_{2,p}(r, \nu, \eta_m)\right) \tag{35}$$

The function $\bar{\bar{G}}_{2,p}$ is defined as the transformation of $G_{2,p}$ in the ϕ and z directions, by the CITT procedure, and is given by Eq. (36). The function $\bar{\bar{\xi}}_p$ gives the transformation of the orthonormal basis system ξ_p in the ϕ and z directions.

$$\bar{\bar{G}}_{2,p}(r, \nu, \eta) = \bar{\bar{\xi}}_p \frac{J_\nu(r\eta_m)(Y_{\nu-1}(r_1\eta_m) - Y_{\nu+1}(r_1\eta_m)) - (J_{\nu-1}(r_1\eta_m) - J_{\nu+1}(r_1\eta_m))Y_\nu(r\eta_m)}{J_\nu(r_2\eta_m)(Y_{\nu-1}(r_1\eta_m) - Y_{\nu+1}(r_1\eta_m)) - (J_{\nu-1}(r_1\eta_m) - J_{\nu+1}(r_1\eta_m))Y_\nu(r_2\eta_m)} \tag{36}$$

Using the same procedure used for the first auxiliary problem, considering the boundary conditions of the physical problem given by Eqs. (3)-(10), and the boundary conditions of the second auxiliary problem given by Eqs. (30)-(34), we obtain:

$$k_2 \int_{\Gamma_2} \left[G_{2,p}\frac{h_2}{k_2}(Y - T_\infty) - Y\frac{\partial G_{2,p}}{\partial \boldsymbol{n}_2}\right] d\Gamma_2 = -\int_{\Gamma_1} k_2\, G_{2,p}\frac{\partial T_2}{\partial \boldsymbol{n}_2}\, d\Gamma_1 \tag{37}$$

The left side of Eq. (37) is defined as $k_2 \mathcal{R}(G_{2,p,k})$, where $\mathcal{R}(\ )$ is the reciprocity functional. Then, it is possible to rewrite this expression as:

$$k_2 \mathcal{R}(G_{2,p}) = \langle G_{2,p}, -k_2\frac{\partial T_2}{\partial \boldsymbol{n}_2}\rangle_{\Gamma_1} \tag{38}$$

We assume, in Eq. (38), that interfacial heat flux can be written as a linear combination of the orthogonal functions γ_i, as described in Eq. (39), where γ_i is defined as in Eq.(40), and δ_i are the weighting coefficients to be determined.

$$\left(-k_2 \frac{\partial T_2}{\partial \boldsymbol{n}_2}\right)_{\Gamma_1} = \sum_{i=1}^{M} \delta_i \gamma_i \tag{39}$$

$$\gamma_i = \left(G_{2,i}\right)_{\Gamma_1} \tag{40}$$

Then, combining Eqs. (38) and (39) we can write the following linear system to determine δ_i:

$$k_2 \mathcal{R}\left(G_{2,p}\right) = \sum_{i=1}^{M} \delta_i \langle \gamma_i, \gamma_p \rangle_{\Gamma_1} \tag{41}$$

Once δ_i is found, the interfacial heat flux can be determined directly from Eq. (39).

3.3 Expression of the thermal contact conductance

The TCC can be determined in terms of the temperature jump, obtained from Eq. (27), and the interfacial heat flux, given by Eq. (39), through the Eq. (42).

$$h_{ctc} = \frac{\sum_{i=1}^{M} \delta_i \gamma_i}{\sum_{i=1}^{N} \alpha_i \beta_i} \tag{42}$$

4. RESULTS AND DISCUSSIONS

Numerical experiments were made to verify the estimates obtained by the method. The direct problem, described by Eqs. (1)-(10), was solved through the finite difference method (FDM) for a known distribution of h_{TCC} to obtain the exact temperature distribution T_{FDM} on the external surface Γ_2. Then, synthetic temperature measurements, *Y*, were obtained as $Y = T_{\mathrm{FDM}} + \epsilon\sigma$, where σ represents the standard deviation of the measurement and ϵ is a white random Gaussian sequence with unity standard deviation. In this work, three different values of σ were considered to investigate the robustness of the developed method: $\sigma = [0°C, 0.1°C, 0.5°C]$.

In order to perform a quantitative comparison for each case, the root mean squared error (RMSE) was calculated using Eq. (43), where $\boldsymbol{x}$ represents the evaluated quantity by the RMSE, and N_p is the number of considered points in the evaluation

$$RMSE = \sqrt{\frac{1}{N_p} \sum_{i=1}^{N_p} \left(\boldsymbol{x}_{exact,i} - \boldsymbol{x}_{estimated,i}\right)^2} \tag{43}$$

The orthonormal basis functions $\psi_p(\phi, z)$ and $\xi_p(\phi, z)$ were taken as a combination of sines and cosines. These functions can be constructed as a combination of two orthonormal basis functions, where $\psi_p(\phi, z) = \psi_k(\phi) \otimes \psi_l(z)$. The orthonormal functions are defined according to Tougri (2018), given as:

$$\psi_k(\phi) = \begin{cases} \sqrt{\frac{1}{2\pi r_2}} & \text{for } k = 1 \\ \sqrt{\frac{2}{\pi r_2}} \cos\left(\frac{k}{2}\phi\right) & \text{for } k = 2,4,\ldots,\text{even} \\ \sqrt{\frac{2}{\pi r_2}} \sin\left(\frac{k-1}{2}\phi\right) & \text{for } k = 3,5,\ldots,\text{odd} \end{cases} \qquad \psi_l(z) = \begin{cases} \sqrt{\frac{1}{L}} & \text{for } l = 0 \\ \sqrt{\frac{2}{L}} \cos\left(\frac{l\pi}{L} z\right) & \text{for } l = 1,2,3,\ldots \end{cases} \tag{44}$$

For the numerical results, four different specimens were considered, composed of two different materials: 3003Aluminum alloy, which is vastly applied to pipes for food and petroleum industry, having a thermal conductivity of $154[\mathrm{W/mK}]$; and AISI 1020 Carbon Steel, which is used in a wide range of application, with a thermal conductivity of $51.9[\mathrm{W/mK}]$. Table 3 describes the final assembled materials tested.

Since there is no adequate method to justify the existence of an optimum number of orthogonal terms, the selection of the number of terms *N* and *M*, in Eq. (42), for determining the temperature jump and the interfacial heat flux, involves testing a finite number of terms and calculating the relative error of h_{TCC}, that is considered known in this initial analysis. The number of orthogonal functions that result in the lowest relative error is applied to estimate the TCC in the findings of this paper.

Table 3. Configuration of specimens.

Specimen	Inner Pipe Material	Outer Pipe Material
1	Aluminum Alloy 3003	Aluminum Alloy 3003
2	AISI Carbon Steel 1020	AISI Carbon Steel 1020
3	AISI Carbon Steel 1020	Aluminum Alloy 3003
4	Aluminum Alloy 3003	AISI Carbon Steel 1020

Four different configurations of h_{ctc} were considered, all of which have discontinuous shapes, representing potential flaws in the tubes' interfaces. Each shape can be viewed in the "a)" column of Figure 2, which represent the specimen number 1 from Table 3. The different test-cases for the h_{ctc} correspond to the first (test-case 1), second (test-case 2), third (test-case 3) and fourth (test-case 4) rows, respectively. Notice that the exact TCC varies from 0 to $1000[\mathrm{W/m^2K}]$. The "b)" column represents the results considering $\sigma = 0°\mathrm{C}$, "c)" column represents the results considering $\sigma = 0.1°\mathrm{C}$, and the "d)" column represents the results considering $\sigma = 0.5°\mathrm{C}$.

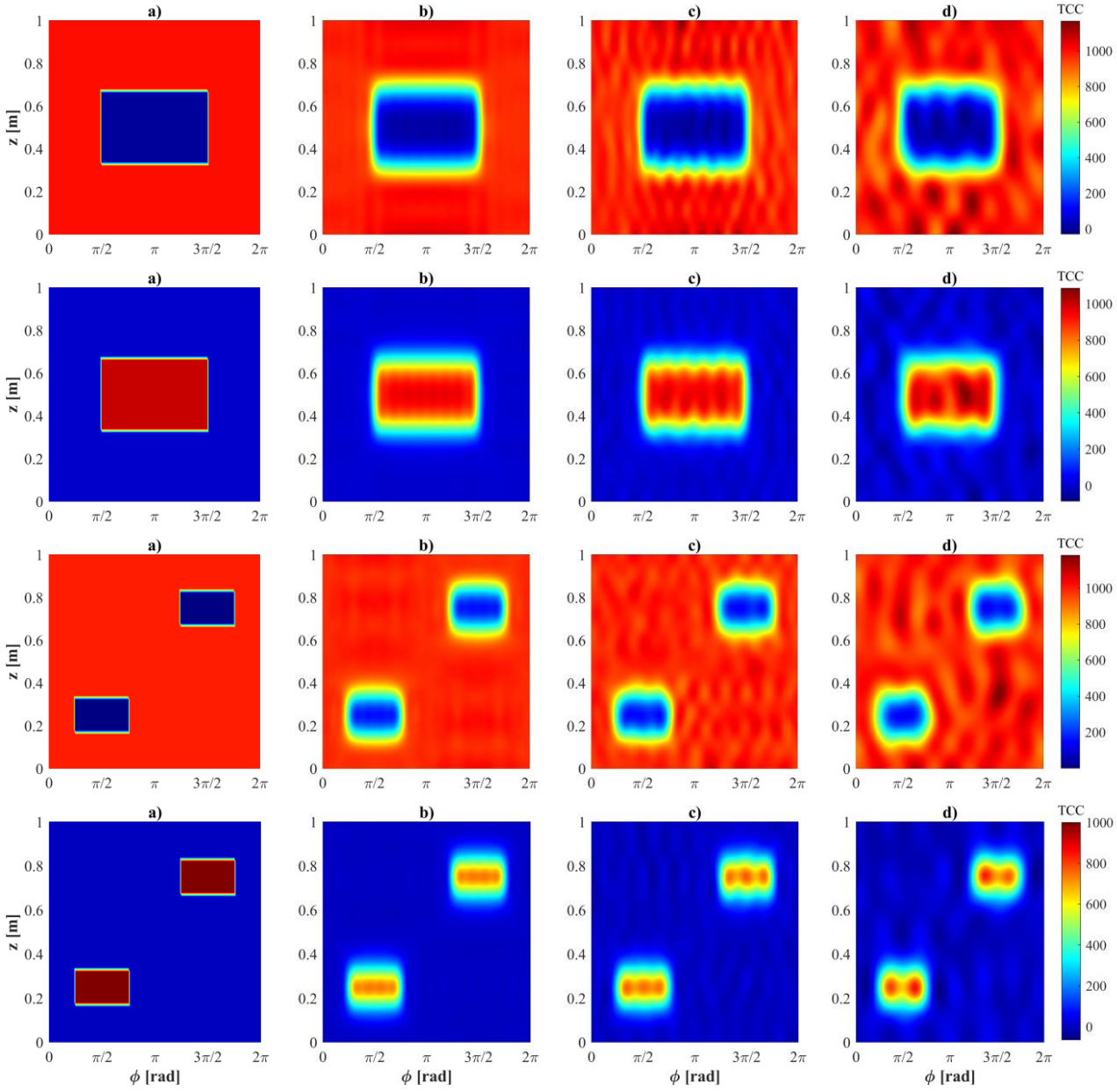

Figure 2. Estimation of h_{TCC} for specimen number 1.

The root mean squared errors ($RMSE$) of the temperature jump, the interfacial heat flux, and the estimated TCC are presented in Table 4, along with the corresponding number of orthonormal functions used for each calculation.

Table 4. *RMSE* and number of orthonormal functions for specimen 1.

CASE	σ [°C]	$RMSE_{\Delta T}$[°C]	$N_{\phi_{\Delta T}}$	$N_{z_{\Delta T}}$	$RMSE_q$[kW/m^2]	N_{ϕ_q}	N_{z_q}	$RMSE_{h_{TCC}}$[W/m^{2}K]
1	0	3.033	28	21	8.890	30	11	136.5
	0.1	3.058	22	9	8.990	26	11	138.6
	0.5	3.261	10	9	9.555	14	11	150.3
2	0	3.088	28	21	9.143	30	13	142.8
	0.1	3.109	22	9	9.239	22	13	143.9
	0.5	3.271	14	9	9.785	14	13	151.2
3	0	2.405	20	21	8.943	28	13	132.9
	0.1	2.426	20	18	9.073	20	13	135.6
	0.5	2.828	12	9	9.462	12	13	145.6
4	0	2.582	24	29	9.421	28	12	143.7
	0.1	2.613	20	21	9.512	20	12	144.6
	0.5	2.770	12	10	9.741	12	10	146.0

It can be observed that, in general, higher noise levels require fewer orthogonal functions to maintain stability. This trend is consistent with previous works that have employed the reciprocity functional method, such as Tougri et. al (2018) and Freitas (2019). Despite the increase in $RMSE$ when noise levels are higher, it is still possible to observe the discontinuous shape in the estimated h_{ctc}. This suggests that even with high noise levels, it remains feasible to detect potential flaws in the specimen through the estimated h_{ctc}.

In Figure 3, the $RMSE_{h_{TCC}}$ divided by the total variation of h_{TCC} ($\Delta h_{TCC} = 1000$[W/m^{2}K]) for each specimen (Sp.) is shown, displaying all h_{TCC} configurations considered (test-cases 1,2,3, and 4), to indicate the errors associated with the estimate. As expected, the *RMSE* increases with the noise levels in all cases. However, it is noteworthy that the $RMSE$ did not show a significant increase for any case, indicating that the solutions remained stable. This stability allows for a qualitative analysis of the presence of flaws in the studied specimens, even under the influence of high noise levels. It is also evident from Figure 3 that, in general, the presence of more than one discontinuity in the specimen (test-cases 3 and 4) does not significantly impact the estimating procedure. The $RMSE$ for these cases are comparable to the cases where only one discontinuity is present (test-cases 1 and 2). This suggests that the methodology can effectively handle multiple discontinuities without a significant loss in accuracy.

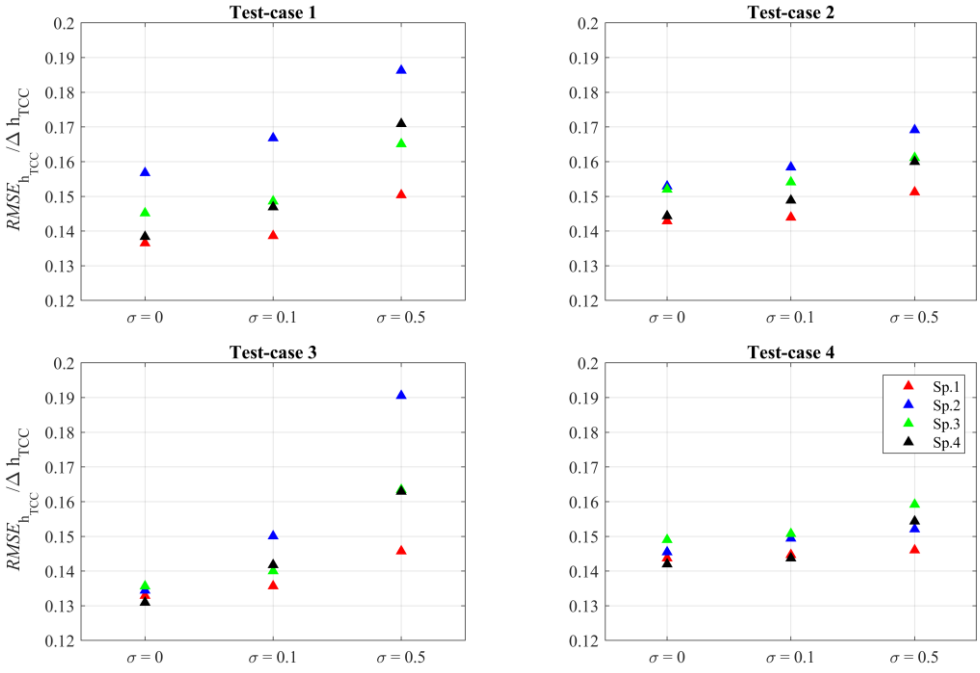

Figure 3. Estimation errors for each test-case.

The results from all different cases in this study demonstrated that the combination of the RF method with the CITT successfully recovered the distribution of the TCC in a three-dimensional steady-state problem, considering cylindrical coordinates, where the TCC configuration varies with the longitudinal and angular directions.

5. CONCLUSIONS

In this paper, the RF method combined with the CITT was applied to a steady-state three-dimensional heat conduction problem in cylindrical coordinates, aiming to estimate four different configurations of spatially varying thermal contact conductances (TCCs) between two contacting solids. Four different specimens were considered composed by two materials with different thermal conductivities.

The method yields an analytical solution for the inverse problem, requiring only the dimensions of the studied body and temperature measurements taken on the outer surface of the tube to estimate the TCC. As a result, it offers a low computational cost and good accuracy. By avoiding the need for intricate numerical simulations or additional data, the approach streamlines the estimation process while maintaining a high level of precision in the results. This advantage makes the method well-suited for practical applications where computational resources and time efficiency are crucial considerations.

Furthermore, the ease of implementation and good accuracy make it a valuable tool for reliably estimating the TCC in a wide range of engineering scenarios. However, the optimum number of orthonormal basis functions considered in the solution should be investigated in future studies, as it can potentially impact the solution's stability. Careful exploration of this aspect ensures the robustness and reliability of the method in various practical applications.

To assess the robustness of the method, we investigated three different noise levels of the measurements. The results obtained from the study demonstrated remarkable agreement with the exact solution, even when high noise levels were introduced. This enabled the identification of regions that potentially contain flaws in the studied body. The technique shown accurate results for the estimated TCCs.

6. ACKNOWLEDGEMENTS

This paper was partially funded by the following Brazilian agencies: CNPq (Conselho Nacional para o Desenvolvimento Científico e Tecnológico), FAPERJ (Rio de Janeiro State Agency for Research), FAPES (Espírito Santo Research and Innovation Support Foundation), ANP-PRH8 (Brazilian National Agency for Oil, Gas and BioFuels – Human Research Program number 8), and Coordenação de Aperfeiçoamento de Pessoal de Nível Superior – Brasil (CAPES) – Finance Code 001.

7. REFERENCES

Andrieux, S., and Abda, A. 1993. "The reciprocity gap: a general concept for flaws identification problems," *Mech. Res. Commun.*, vol. 20, pp. 415-420.

Colaço, M., and Alves, C.J.S. 2012. "Estimation of unknown contact resistance by means of reciprocity function approach", in *Proceedings of the European Congress on Computational Methods in Applied Sciences and Engineering - ECCOMAS* , Vienna, Austria.

Colaço, M.J., and Alves, C.J.S., 2015. "A backward reciprocity function approach to the estimation of spatial and transient thermal contact conductance in double-layered materials using non-intrusive measurements," *Numer. Heat Transfer*, vol. 68, pp. 117-132.

Colaço, M.J., Alves, C.J.S. and Orlande, H. 2014. "Transient non-intrusive method for estimating thermal contact conductance by means of the reciprocity functional approach", *Inverse Prob. Sci. Eng.*, vol. 23, pp. 688-717.

Cui, T., Li, Q., Xuan, Y., , and Zhang, P., 2014. "Multiscale simulation of thermal contact resitance in electronic packing," *International Journal of Thermal Sciences*, vol. 83, pp. 16-24..

Fill, A., Koch, S., Birke, K.P. 2020. "Algorithm for the detection of a single cell contact loss within parallel-connected cells based on continuous resistance ratio estimation". *Journal of Energy Storage.* Vol.27, 1-6.

Freitas, G.C., 2019. "*Estimation of thermal contact conductances in irregular interfaces using the classical integral transform technique and the reciprocity functional method (In Portuguese)*". Master's thesis, Program in Mechanical engineering, Federal University of Rio de Janeiro, Rio de Janeiro, Brasil.

Goudarzi, K., Moosaei, A., & Gharaati, M., 2015. "Applying artificial neural networks (ANN) to the estimation of thermal contact conductance in the exhaust valve of internal combustion engine". *Applied Thermal Engineering*, Vol. 87, p. 688–697.

Guilmore, D. G., 2002. "*Spacecraft Thermal Control Handbook*". 2 ed., El Segundo, CA: The Aerospace Press.

Karthick, K. Suresh, S., Singh, H., Joy, G.C., Dhanuskodi, R. 2019. "Theoretical and experimental evaluation of thermal interface materials and other influencing parameters for thermoelectric generator system". *Renewable Energy. Vol. 134, 25-43.*

Loulou, T., & Scott, E. P., 2006. "An inverse heat conduction problem with heat flux measurements". *International Journal for Numerical Methods in Engineering*, Vol.67(11), 1587–1616.

McWaid, T. H., and Marshall, E., 1992. "Application of the modified greenwood willianson contact modell for the," *Wear*, vol. 152, pp. 263-277.

Milosevic, N. D., Raynaud, M., and Maglic, D., 2002. "Estimation of thermal contact resistance between the materials," *Inverse Problems in Engineering*, vol. 10, pp. 83-103.

Özisik, M., 1993. "*Heat Conduction".* 2ed. John Wiley & Sons, New York.

Padilha, R., Colaço, M.J., Orlande, H., Abreu, L. 2016. "*An analytical method to estimate spatially-varying thermal contact conductances using the reciprocity functional and the integral transform methods: Theory and experimental validation*". International Journal of Heat and Mass Transfer, vol. 100, pp. 599-607.

Tougri, I., 2018. "*Convection heat transfer coefficient estimation in ducts using the reciprocity functional method"*. Ph.D. thesis, Program in Mechanical Engineering, Federal University of Rio de Janeiro, Rio de Janeiro, Brasil.

Tougri, I., Colaço, M.J., Bozzoli, F., Cattani, L.,2018. "Internal heat transfer coefficient estimation in three-dimensional ducts through the reciprocity functional approach – An analytical approach and validation with experimental data*". International Journal of Heat and Mass Transfer*, Vol. 122, p.587-601.

8. RESPONSIBILITY NOTICE

The authors are the only responsible for the printed material included in this paper.